HHS Public Access

Author manuscript

Eur J Neurosci. Author manuscript; available in PMC 2016 September 01.

Published in final edited form as:

Eur J Neurosci. 2015 September ; 42(6): 2271–2282. doi:10.1111/ejn.12996.

The retrotrapezoid nucleus stimulates breathing by releasing glutamate in adult conscious mice

Benjamin B. Holloway, **Kenneth E. Viar**, **Ruth L. Stornetta**, and **Patrice G. Guyenet**

Department of Pharmacology, University of Virginia, Charlottesville, VA 22908

Abstract

The retrotrapezoid nucleus (RTN) is a bilateral cluster of neurons located at the ventral surface of the brainstem below the facial nucleus. RTN is activated by hypercapnia and stabilizes arterial PCO_2 by adjusting lung ventilation in a feedback manner. RTN neurons contain *Vglut2* transcripts (vesicular glutamate transporter-2, *Slc17a6)*, and their synaptic boutons contain Vglut2 immunoreactivity. Here, we use optogenetics to test whether RTN increases ventilation in conscious adult mice by releasing glutamate.

Neurons located below the facial motor nucleus were transduced unilaterally to express channelrhodopsin-2-(ChR2-)eYFP using lentiviral vectors that employ the Phox2b-activated artificial promoter, PRSx8. The targeted population consisted of two types of Phox2b-expressing neurons: non-catecholaminergic neurons (putative RTN chemoreceptors) and catecholaminergic (C1) neurons. Opto-activation of a mix of ChR2-expressing RTN and C1 neurons produced a powerful stimulus frequency-dependent (5-15 Hz) stimulation of breathing in control conscious mice. Respiratory stimulation was comparable in mice in which dopamine-*β*-hydroxylase-positive ($D\beta H^{+}$) neurons no longer expressed Vglut2 ($D\beta H^{Cre/0};;Vglut2^{fl/fl}$). In a third group of mice, we injected a mixture of PRSx8-Cre lentiviral vector and a Cre-dependent ChR2-AAV2 unilaterally into RTN of $D\beta H^{+/+};;Vglut2^{fl/fl}$ mice; this procedure deleted *Vglut2* from ChR2-expressing neurons regardless of whether or not they were catecholaminergic. The ventilatory response elicited by phostimulation of $ChR2^{+}$ neurons was virtually absent in these mice. Resting ventilatory parameters were identical in the three groups of mice and their brains contained similar numbers of $ChR2^{+}$ catecholaminergic and non-catecholaminergic neurons. From these results we conclude that RTN neurons increase breathing in conscious adult mice by releasing glutamate.

Abstract

Address correspondence to: Patrice G. Guyenet, PhD, University of Virginia Health System, P.O. Box 800735, 1340 Jefferson Park Avenue, Charlottesville, VA 22908-0735. Tel: (434) 924-7433; Fax: (434) 982-3878; pgg@virginia.edu.

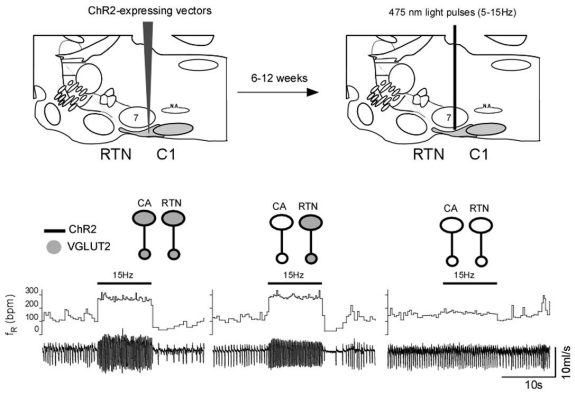

Keywords

breathing; central respiratory chemoreceptors; glutamate; optogenetics

Introduction

The retrotrapezoid nucleus (RTN) contributes to arterial PCO_2 stability by regulating breathing frequency and amplitude in a feed-back manner (Mulkey *et al.*, 2004; Abbott *et al.*, 2009; Guyenet *et al.*, 2010; Marina *et al.*, 2010; Basting *et al.*, 2015). Activation of these neurons by CO_2 *in vivo* is now attributed to their intrinsic pH-sensitivity, paracrine influences from surrounding pH-responsive astrocytes, and inputs from the carotid bodies and other CO_2-responsive CNS neurons (Gourine *et al.*, 2010; Hodges & Richerson, 2010; Huckstepp *et al.*, 2010; Nattie & Li, 2010; Hawryluk *et al.*, 2012; Wang *et al.*, 2013a; 2013b; Kumar *et al.*, 2015).

RTN neurons may use glutamate as a transmitter because they contain *Vglut2* transcripts and their axonal varicosities are Vglut2-immunoreactive (Mulkey *et al.*, 2004; Bochorishvili *et al.*, 2012). However, the CNS is replete with Vglut2-expressing neurons in which transmitters other than glutamate seem to play the dominant role (e.g. orexinergic neurons, neuroendocrine cells in hypothalamus, dopaminergic neurons)(Lin *et al.*, 2003; Rosin *et al.*, 2003; Stuber *et al.*, 2010; Van den Pol, 2012). Further, many RTN neurons also express galanin, a typically inhibitory peptide (Pieribone *et al.*, 1998; Stornetta *et al.*, 2009; Bochorishvili *et al.*, 2012). The present study seeks more definitive evidence that RTN neurons activate breathing by releasing glutamate in conscious adult mice.

Opto- and pharmacogenetic experiments have been instrumental in showing that RTN neurons activate breathing in rats (Abbott *et al.*, 2009; Marina *et al.*, 2010; Abbott *et al.*, 2011). In these experiments the actuator (opsin or allatostatin receptor) was introduced into RTN neurons using lentiviral vectors whose selectivity relies on a Phox2b-sensitive promoter, PRSx8 (Hwang *et al.*, 2001). However, since Phox2b is expressed by both RTN and neighboring catecholaminergic (CA) neurons, such vectors cause transgene expression in both CA cells and the RTN (Stornetta *et al.*, 2006).

Lower brainstem catecholaminergic cells, unlike RTN neurons, express dopamine-β-hydroxylase (DβH) and can be specifically targeted in DβH$^{Cre/0}$ mice (Abbott *et al.*, 2014). ChR2-mediated stimulation of these lower brainstem catecholaminergic neurons increases breathing unless vesicular glutamate transporter-2 (*Vglut2, Slc17a6*) (Takamori *et al.*, 2000) is selectively knocked out of these cells (Abbott *et al.*, 2014). Therefore these catecholaminergic neurons increase breathing by releasing glutamate (Abbott *et al.*, 2014).

To determine whether glutamate is the primary transmitter of RTN neurons *in vivo* we used ChR2-based optogenetics to activate RTN and catecholaminergic neurons in mice in which Vglut2 was expressed by both cell types or in mice in which *Vglut2* exon2 was selectively excised from the CA cells or excised from both CA and RTN neurons. *Vglut2* exon2 excision from both CA and RTN neurons was achieved by targeted injections of a Cre-expressing PRSx8 promoter-driven vector in *Vglut2$^{(flox/flox)}$* mice (Tong *et al.*, 2007; Kaur *et al.*, 2013). Selective *Vglut2* exon2 excision from the CA neurons was achieved by crossing *DβH$^{Cre/0}$* mice with *Vglut2$^{fl/fl}$* mice. In all mice, we photostimulated the ChR2-transduced neurons and measured their breathing responses using whole body plethysmography.

Materials and Methods

Animals

Animal use was in accordance with the NIH Guide for the Care and Use of Laboratory Animals and approved by the University of Virginia Animal Care and Use Committee. *DβH$^{Cre/0}$* mice were obtained from the Mutant Mouse Regional Resource Center at the University of California, Davis, CA, USA [Tg(DβH-cre)KH212Gsat/Mmcd; stock # 032081-UCD] and maintained as hemizygous (Cre/0) on a C57BL/6J (C57) background. Homozygous *Vglut2$^{flox/flox}$* mice (JAX Stock #012898; STOCK *Slc17a6$^{tm1Lowl/J}$*)(Tong *et al.*, 2007) were bred with *DβH$^{Cre/0}$* mice to generate *DβH$^{Cre/0}$; Vglut2$^{flox/0}$* mice and subsequently crossed with *Vglut2$^{flox/flox}$* mice to generate *DβH$^{Cre/0}$; Vglut2$^{flox/flox}$* and *DβH$^{0/0}$; Vglut2$^{flox/flox}$* (Depuy *et al.*, 2013). C57BL/6J(C57, JAX Stock#000664) mice were used in control experiments.

Experimental design

The experimental design is summarized in Table 1. The experiments are predicated on the following two assumptions that are supported by prior experiments in rats and mice and were verified here by a detailed histological analysis of every mouse that was used. First, the transgene of PRSx8 promoter-containing LVV (Cre or ChR2-eYFP) is selectively expressed in Phox2b-containing neurons (Abbott *et al.*, 2009; Basting *et al.*, 2015). Second, at the ventral surface of the medulla oblongata, the Phox2b-containing neurons consist almost exclusively of catecholaminergic and RTN chemoreceptor neurons. The rostral ventrolateral medullary catecholaminergic neurons (C1 neurons) and RTN neurons contain *Vglut2* transcripts (Stornetta *et al.*, 2006; Abbott *et al.*, 2014). Therefore when we injected PRSx8 Cre LVV together with a Cre-dependent ChR2 AAV in the rostral ventral medulla of C57 mice, we produced ChR2 expression in both catecholaminergic and RTN neurons and both cell types expressed Vglut2 (Group 1). To isolate the breathing effects resulting specifically from RTN stimulation, we injected PRSx8-ChR2 in *DβH$^{Cre/0}$;Vglut2$^{fl/fl}$* mice, and therefore

also produced expression of ChR2 in both cell types but Vglut2 was deleted in the CA neurons only (Group 2) (Abbott *et al.*, 2014). Finally, in order to test whether glutamate is responsible for the breathing stimulation elicited by RTN neuron activation, we injected a mixture of PRSx8 Cre LVV and a Cre-dependent ChR2 AAV into the RTN region of *Vglut2*$^{fl/fl}$ mice. In this case both CA and RTN were transduced with Cre and, the neurons that expressed ChR2 should no longer express Vglut2 because the recombinase should also have excised the *Slc17a6* exon2. In summary, if RTN stimulation drives breathing by releasing glutamate, the prediction is that photostimulation of ChR2-expressing neurons should produce robust breathing stimulation in groups 1 (C57) and 2 (*DβH*$^{Cre/0}$;*Vglut2*$^{fl/fl}$) and little or no breathing stimulation in group 3 (*Vglut2*$^{fl/fl}$).

Unilateral viral vector injection and optical fiber implantation

The following viral vectors were used in these experiments: PRSx8-ChR2(H134R)-eYFP lentiviral vector (LVV, stock: 1.2×10^9 viral particles/ml), PRSx8-Cre LVV (stock: 5.4×10^9 viral particles /ml) and DIO-ChR2-eYFP AAV2; stock: 3.0×10^{12} viral particles/ml). PRSx8 is a Phox2b-activated promoter that restricts transgene expression to cells that express high levels of this transcription factor (Hwang *et al.*, 2001). When PRSx8-containing LVV is injected accurately into RTN, transgene expression is restricted to Phox2b-immunoreactive neurons that reside at the ventral surface of the medulla oblongata (Stornetta *et al.*, 2006; Abbott *et al.*, 2009; Marina *et al.*, 2010). Non-neuronal cells, including astrocytes, are not transduced (Basting *et al.*, 2015). The transduced neuronal population includes catecholaminergic neurons (C1 and A5 neurons) and non-catecholaminergic neurons, both of which contain *Vglut2* transcripts (Stornetta *et al.*, 2002; Lazarenko *et al.*, 2009). Recordings performed in Phox2b-eGFP transgenic mice have shown that the vast majority of the non-catecholaminergic Phox2b+ population of neurons located below the facial motor nucleus (~95% in slices and ~80% after complete dissociation) are activated by acidification (Lazarenko *et al.*, 2009; Wang *et al.*, 2013b). In addition, the respiratory stimulation contributed by the same group of Phox2b+ neurons is strikingly dependent on arterial pH in conscious rats (Basting *et al.*, 2015). For these and other reasons (Guyenet, 2014), we refer to these Phox2b+ non-aminergic neurons as RTN chemoreceptors. Ten adult *DβH*$^{Cre/0}$; *Vglut2*$^{flox/flox}$ mice (10-20 wks; 6 females, 4 males) received injections of PRSx8-ChR2-eYFP LVV (stock diluted 5 fold in sterile Dulbecco's phosphate buffered saline). A 1:15 (v/v) mixture of PRSx8-Cre LV stock and DIO-ChR2-eYFP AAV2 stock was injected into 8 C57 mice (7-11 wks; 1 female, 7 males) and in 9 *DβH*$^{0/0}$; *Vglut2*$^{flox/flox}$ mice (7-11 wks; 5 females, 4 males).

Vector microinjection and implantation of optical fibers were performed under aseptic conditions in mice anesthetized with a mixture of ketamine (100 mg/kg) and dexmedetomidine (0.2 mg/kg; i.p.) as previously described (Abbott *et al.*, 2013). Adequate anesthesia was judged by the absence of the corneal and hind-paw withdrawal reflex. Additional anesthetic was administered if necessary (20% of the original dose, i.p.). Anesthetized mice were placed into a modified stereotaxic device (Kopf) and maintained at 37°C on a thermostatically controlled heating pad. Three 120 nl injections of PRSx8-ChR2-eYFP LVV or PRSx8-Cre LVV/DIO-ChR2-eYFP AAV2 mixture were aligned 0.2 mm apart in the rostrocaudal direction and located 1-4-1.5 mm lateral to the midline and 100 μm

below the left facial motor nucleus. The lower boundary of this nucleus was identified electrophysiologically with antidromic field potentials as described previously (Abbott *et al.*, 2014).

Following microinjection of the viral vector(s), a 125 μm-diameter fiber optic, consisting of a stripped, glass-clad multimode optical fiber (105 μm-core, 0.22 numerical aperture; Thorlabs, Newton, NJ, USA) glued into a zirconia ferrule (1.25 mm O.D., 126 μm bore; Precision Fiber Products, Milpitas, CA, USA), was placed with its tip ~100 μm above the injection site. The fiber optic ferrule was secured to the skull with adhesive (Loctite 3092). Mice received post-operative boluses of atipamezole (α_2-adrenergic antagonist, 2 mg/kg, s.c.), ampicillin (125 mg/kg, i.p.), and ketoprofen (4 mg/kg, s.c.). Ampicillin and ketoprofen were re-administered 24 hours post-operatively.

Combination optogenetics and whole-body plethysmography in conscious mice

Photostimulation of the ChR2-transduced neurons was performed as previously described (Abbott *et al.*, 2014). Prior to implantation, the light output of each implanted optical fiber was measured with a light meter (Thorlabs) and the laser setting was adjusted to deliver ~9 mW. This setting was later used during the experiments. Photostimulation and plethysmography trials were carried out 6-12 wks after viral injections. Breathing parameters were measured in conscious mice using unrestrained whole-body plethysmography (EMKA Technologies, Falls Church, VA ,USA) as previously described (Abbott *et al.*, 2014). The breathing parameters measured were breathing frequency (f_R in breaths/minute, bpm), tidal volume (V_T in μl/g) and minute volume (V_E in ml/(min × g). Before being placed in the plethysmography chamber, the mice were briefly anesthetized with isoflurane while the connection between the implanted optical fiber and the laser delivery system was established. Airflow signals were calibrated to air injected via a 1mL syringe. Tidal volume was determined by the area under the curve during inspiratory breaths divided by weight. The chamber was continuously flushed with dry, room-temperature air delivered at 0.5 liter/min. Chamber pressure signals were detected via a differential pressure transducer, amplified (× 500), band pass filtered (0.25Hz to 35Hz), and digitized at greater than 100 Hz with Spike 2 software (v7.10, Cambridge Electronic Design, Ltd., Cambridge, UK). Respiratory frequency (f_R; breaths/min) was analyzed exclusively during periods of behavioral quiescence. To evaluate the effects of photostimulation on f_R, 10 s-long trains of 5 ms light pulses were delivered at three frequencies (5, 10 and 15 Hz). Behavioral quiescence was determined by direct observation or via an automated function using Spike2 software. For automated acquisition, laser stimulation was triggered at one of three frequencies (5 Hz, 10 Hz, 15 Hz), as determined by a random number generator, after an eleven second period of breathing in which max and min f_R were less than 200 bpm and greater than 90 bpm, no sighing occurred, mean f_R was between 130 and 170 bpm, and the preceding stimulation had occurred at a time greater than 60 s prior. All stimulation trials were visually inspected posthoc and only those trials that had occurred during behavioral quiescence were used for analysis. The reported changes in f_R reflect the average response of 5-10 trials per mouse at each stimulation frequency.

Histological procedures

At the end of experimental procedures in conscious mice, animals were anesthetized with an overdose of pentobarbital and perfused transcardially with 10-15 ml of phosphate buffered saline followed by 75-100 ml of 3% paraformaldehyde. Brains were extracted and post-fixed for 24-72 hours before sectioning on a vibrating microtome at room temperature. Thirty micron coronal sections throughout the medulla/pons were collected into cryoprotectant solution (30% ethylene glycol, 20% glycerol, 50% 100 mM sodium phosphate buffer, pH 7.4) and stored at −20°C until further processing.

One-in-three series of coronal sections were processed free floating for detection of Phox2b, eYFP and tyrosine hydroxylase (TH) by immunohistochemistry as previously described (Abbott *et al.*, 2011). Briefly, sections were incubated simultaneously in antibodies directed against Phox2b (rabbit; 1:8000, generously provided by J.F. Brunet (Institut de Biologie de l'Ecole normale supérieure, Paris, France), TH (sheep; 1:2000, EMD Millipore, Billerica, MA) and eYFP (chicken; 1:2000, AVES labs, Tigard, OR). The specificity of the Phox2b antibody has been established previously by demonstrating that *Phox2b* transcripts and Phox2b immunoreactivity are co-localized (Pattyn *et al.*, 1997) and that immunoreactivity is absent in Phox2b knock-out mice (Dubreuil *et al.*, 2009). After 24- 48 hours, sections were rinsed and incubated in secondary antibodies at 1:200 (anti-rabbit-biotin tagged IgG; anti-sheep IgG tagged with DyLight 647; anti-chicken IgY tagged with Alexa 488; all secondaries from Jackson ImmunoResearch, West Grove, PA) rinsed and incubated in streptavidin-HRP (1:200; Perkin-Elmer, Melville, NY). Rinsed and incubated in tyramide-Cy3 (1:200; Perkin-Elmer), then rinsed and mounted onto slides, dehydrated through alcohols and xylenes and covered with DPX mountant (Electron Microscopy Sciences, Hatfield, PA).

Sections were examined and cell distributions mapped with a computer-driven stage and Neurolucida software (v. 11, MBF Bioscience, Wiliston, VT) attached to a Zeiss Axioskop widefield fluorescence microscope (Carl Zeiss Microscopy, Thornwood, NY) using 20X (NA= 0.17) or 100x (oil, NA=1.4) objectives and images recorded with a Zeiss MRC rev. 3 CCD camera (1388×1040 pixels; Carl Zeiss Microscopy). Some images were rendered from maximum intensity projections of z-stacks captured at 0.3 micron intervals through 10-15 micron depth of tissue, then deconvolved through 7 iterations using the automatic 3D blind deconvolution in AutoQaunt X3 software (Media Cybernetics, Rockville, MD). Images were imported into Canvas software (v. 10, ACD Systems, Seattle, WA), levels adjusted over the entire image to include all information containing pixels and assembled into figures.

Statistical analysis

Data were analyzed by one or two-way ANOVA with repeated measures with differences between groups determined using Sidak multiple comparisons using the PRISM software (GraphPad PRISM Version 6). Assumptions of the two-way ANOVA were tested with the Shapiro-Wilk test for normality on error residuals for both between and within subjects (R statistical software package version 3.2.0; R Core Team, 2013). Assumptions of the one-way ANOVA for normality were also confirmed with the Shapiro-Wilk test. Power was calculated using R software. The PRISM software tests for sphericity and generates a value

for Geisser-Greenhouse epsilon if sphericity cannot be assumed. In such cases, the fractional df values used to compute a *P* value would be reported (this was not the case for any of our analyses). Test statistics where $P < 0.05$ were considered significant.

Results

Breathing responses elicited by ChR2 photostimulation

The light was delivered for 10 s at 5, 10 and 15 Hz in random order. This frequency range was selected because, in anesthetized rats, these neurons rarely discharge above 12 Hz when exposed to high levels of CO_2 (Guyenet *et al.*, 2005). In groups 1 and 2, in which RTN presumably expressed Vglut2, photostimulation produced a robust frequency-dependent rise in breathing rate (f_R) and tidal volume (V_T) (representative example in Fig. $1A_{1\text{-}4}$, $B_{1\text{-}4}$). By contrast, virtually no effect was observed in group 3, in which Vglut2 was deleted from both ChR2-expressing CA and RTN neurons (Fig. $1C_{1\text{-}4}$). Of note, the breathing stimulation observed in groups 1 and 2 was instantaneous and its amplitude was also instantly maximal consistent with the release of a fast-acting transmitter.

Group data for f_R, V_T, and minute volume V_E are shown in Figures 2, 3 and 4, respectively. The groups were first analyzed for differences in baseline breathing using one-way ANOVA with baseline values averaged across all three stimulation frequencies. There was no significant main effect of group for baseline values of fR, V_T or V_E (see Table 2 for Shapiro-Wilk test of normality and Table 3 for *F* values). The power of this test was 0.93 for f_R, 0.99 for V_T and 0.99 for V_E (all with *P* set at 0.05). In short, there was no difference in baseline breathing variables between the three groups of mice.

Each mouse group was then analyzed separately with 2-way ANOVA with RM for both main effects of photostimulation and frequency of photostimulation (5, 10, 15 Hz) on f_R, V_T and V_E. In groups 1 and 2, in which RTN contained Vglut2, photostimulation produced a robust frequency-dependent increase in f_R, V_T and V_E (significant main effect of both photostimulation and stimulation frequency on f_R, V_T and V_E; see Shapiro-Wilk tests for normality in Table 2 and Table 3 for *F* values). By contrast, there was no effect of stimulation frequency in group 3 and only a small but statistically significant main effect of photostimulation (Tables 2 and 3).

To determine whether optogenetic stimulation had a different effect between the three groups of mice, we first tried a mixed factorial design two-way ANOVA for groups × stimulation frequency with RM on stimulation frequency, and we measured the change (delta) in breathing variables between baseline and stimulation. For V_E this analysis revealed significant differences both between groups and between stimulation frequencies (Table 2 and 3; results of Tukey's multiple comparison tests shown in Fig. 4D). The assumptions of normality on error residuals were not met for f_R and V_T (see Table 2) so the factor of different stimulation frequencies was not examined and data were analyzed on all variables at the 15 Hz stimulation frequency by one-way ANOVA on groups. There was a significant effect of groups (see Tables 2, 3 for assumptions of normality and F stats). Post hoc Tukey's multiple comparison tests showed a highly significant difference for f_R, V_T and V_E between groups 1 and 3 and groups 2 and 3 but no difference between groups 1 and 2

(see Table 4). The statistically non-significant differences between groups 1 and 2 have 95% confidence intervals that span zero and are outside of the 95% confidence intervals for differences between groups 1 and 2 and group 3 for both f_R and V_E (although there was some overlap of the 95% confidence intervals for V_T). Thus, we conclude that the effect of stimulation on breathing was much greater in groups 1 and 2 than in group 3 and that, at least for f_R and V_E, there was no difference between groups 1 and 2.

The observed results are therefore consistent with the hypothesis that selective activation of RTN neurons produces breathing stimulation only if these neurons express Vglut2.

Histology

The first series of histological experiments was designed to verify that, in mice, injections of PRSx8-based lentiviral vectors (PRSX8-ChR2-eYFP LVV or mix of PRSX8-Cre LVV and DIO-ChR2-eYFP AAV2) into the RTN region cause expression of ChR2 selectively in Phox2b-expressing neurons. In two $D\beta H^{Cre/0};;Vglut2^{fl/fl}$ mice injected with PRSX8-ChR2-eYFP LVV, and three $Vglut2^{fl/fl}$ mice injected with mix of PRSX8-Cre LVV and DIO-ChR2-eYFP AAV2, 94.4 ± 1.7 % of transduced (eYFP-expressing) neurons had a Phox2b-immunoreactive nucleus (Fig. 5A-C). This population included 26.1 ± 5.5% TH-immunoreactive, i.e. catecholaminergic neurons (average for the five mice). Thus, in mice as in rats, LVVs with the PRSx8 promoter transduce Phox2b-immunoreactive neurons selectively when these vectors are targeted to the brain region of interest.

The second goal was to ascertain that the number and distribution of the ChR2-transduced neurons was comparable in the three groups of mice. The ChR2-eYFP transduced neurons were located superficially within the ventrolateral medulla from just caudal to the facial motor nucleus caudally to the level of the exit of the facial nerve. The rostrocaudal distribution of the transduced catecholaminergic or non-catecholaminergic (i.e. RTN) neurons was similar in all three groups (Fig. 5E,F). The total number of RTN neurons was estimated by multiplying the cell counts in a one in three series of sections by three and was not different between groups (C57, 195 ± 17.5; $D\beta H^{Cre/0};;Vglut2^{fl/fl}$, 261 ± 50.8; $Vglut2^{fl/fl}$, 201 ± 16.7; one-way ANOVA, $F_{2,20} = 1.549$, $P = 0.237$; Shapiro-Wilk, $W = 0.9282$, $P = 0.09989$; power at α 0.05 = .9448; Fig. 5D). The total number of catecholamine cells transduced was comparable in each group, though group 1 contained fewer transduced CA neurons than did group 2 (C57, 98.1 ± 15.0; $D\beta H^{Cre/0};;Vglut2^{fl/fl}$, 178 ± 10.3; $Vglut2^{fl/fl}$, 158.1 ± 30.3; $F_{2,20} = 4.575$, $P = 0.0231$; Shapiro-Wilk, $W = 0.9302$, $P = 0.1106$; power at α 0.05 = .999; Fig. 5D). Finally, the percentage of RTN neurons in total transduced neurons was also similar (C57, 67 ± 4%; $D\beta H^{Cre/0};;Vglut2^{fl/fl}$, 57 ± 5%; group $Vglut2^{fl/fl}$, 58 ± 4%; one-way ANOVA, $F_{2,20} = 1.717$, $P = 0.205$; Shapiro-Wilk, $W = 0.95083$, $P = 0.3045$; power at α 0.05 = 0.9636).

RTN neurons innervate abundantly the ventral respiratory column, including the preBötzinger Complex, a subdivision of this column that is essential for breathing rate generation (Bochorishvili *et al.*, 2012; Feldman *et al.*, 2013; Kam *et al.*, 2013). We therefore examined the eYFP-labeled nerve terminals located within this region of the medulla oblongata in groups 1 and 3 to verify that *Vglut2* was present in group 1 and had been effectively knocked out from the ChR2-transduced neurons in group 3. These projections are

largely ipsilateral therefore only one side (the left) was examined. In group 1 (N = 3 mice) 89 ± 1% of eYFP-positive terminals counted (avg. 235 terminals counted per mouse) also contained detectable Vglut2-immunoreactivity whereas in group 3 (N = 3; avg. 246 terminals counted per mouse) only 9 ± 1.6% eYFP terminals were Vglut2-immunoreactive (Fig. 6A, RTN projections).

In order to confirm that Vglut2 was appropriately deleted from the RTN neurons in group 3, we used double-label immunohistochemistry and examined eYFP-labeled nerve terminals located in the ventral respiratory column (VRC). In contrast to terminals in VRC from group 1, terminals in this same area from group 3 lacked Vglut2 immunoreactivity (Fig. 6A). We used triple-label immunohistochemistry to determine that *Vglut2* was appropriately deleted from CA neurons in groups 2 and 3 but not in group 1. We examined the raphe pallidus, which receives projections from the CA neurons but not from RTN. Terminals were considered to originate from the CA neurons if they were eYFP+ and TH+ (Abbott *et al.*, 2014). As illustrated in Figure 6B (CA projections), eYFP-positive terminals were TH-negative and Vglut2-positive in C57 mice (group 1) but these terminals lacked Vglut2 immunoreactivity in both the $D\beta H^{Cre/0};;Vglut2^{fl/fl}$ mice (group 2) and the $Vglut2^{fl/fl}$ mice injected with both PRSX8-Cre and ChR2-eYFP AAV2 (group 3).

Discussion

The presence of *Vglut2* transcripts in RTN neurons has been identified previously by *in situ* hybridization and by single cell PCR in rats and mice (Mulkey *et al.*, 2004; Lazarenko *et al.*, 2010). Vglut2 immunoreactivity has also been detected in the axonal varicosities of these neurons (Bochorishvili *et al.*, 2012). Here, we show that Vglut2 expression by RTN neurons is required for these neurons to stimulate breathing in conscious adult mice. These results strongly suggest that glutamate is the main transmitter used by this particular group of chemoreceptors to increase breathing.

RTN neurons: definition and function

The retrotrapezoid nucleus has been variously defined over the years ((Smith *et al.*, 1989; Onimaru & Homma, 2003; Dubreuil *et al.*, 2009) for reviews see (Guyenet *et al.*, 2012; Guyenet, 2014). As in our previous publications, RTN neurons are defined here as a small collection (~800 in mice, ~2000 in rats) of Phox2b-positive non-catecholaminergic and non-cholinergic neurons located under the facial motor nucleus (Stornetta *et al.*, 2006). All of these neurons contain *Vglut2* transcripts, specific proton receptors (Kumar *et al.*, 2015) and lack markers of GABA or glycine neurotransmission (Mulkey *et al.*, 2004; Lazarenko *et al.*, 2009). Half of them also express galanin (Lazarenko *et al.*, 2009; Stornetta *et al.*, 2009). RTN neurons as defined above are probably identical to a cluster of similarly located *Vglut2*-expressing neurons that have been identified by genetic lineage studies as *Atoh1/egr-2/phox2b*-derived (Dubreuil *et al.*, 2009; Ramanantsoa *et al.*, 2011; Ruffault *et al.*, 2015). **The vast majority of** RTN neurons are activated by acid *in vitro* and by hypercapnia *in vivo* (Mulkey *et al.*, 2004; Lazarenko *et al.*, 2010; Basting *et al.*, 2015). RTN neurons express two proton detectors (TASK-2 and a G-protein coupled receptor, GPR4); genetic elimination of each protein separately attenuates the pH-sensitivity of RTN neurons and

reduces the hypercapnic ventilatory reflex by 65% whereas genetic elimination **of both proteins substantially** eliminates both **RTN neuron** pH-sensitivity and the hypercapnic ventilatory reflex **(>85% reduction)** (Gestreau *et al.*, 2010; Wang *et al.*, 2013a; Kumar *et al.*, 2015). RTN neurons selectively innervate the pontomedullary regions that contain the respiratory rhythm and pattern generator and their selective activation increases breathing (Abbott *et al.*, 2009). RTN neurons also receive input from various types of CNS neurons that contribute to the hypercapnic ventilatory reflex (serotonergic, noradrenergic and orexinergic)(reviewed in (Guyenet, 2014)). In short, RTN neurons are both central respiratory chemoreceptors and a nodal point for the chemoreflexes ((Hodges & Richerson, 2010; Li & Nattie, 2010), for recent review: (Guyenet, 2014)).

Contribution of Vglut2 rostroventrolateral medullary CA neurons to breathing

We showed previously that the increased breathing elicited by stimulation of the C1 neurons (catecholaminergic neurons located in the rostral medulla) required expression of Vglut2 by these neurons (Abbott *et al.*, 2014). Therefore, one could have expected more robust respiratory changes in control mice (group 1) than in group 2 in which the C1 cells lack Vglut2. However, this outcome was not found and breathing stimulation was identical in these two groups of mice at all stimulation frequencies. This outcome can be reasonably explained as follows. In our previous study the ChR2-expressing vector was administered more caudally in the ventrolateral medulla to deliberately target the largest possible number of C1 cells and, as a result, around 400 C1 cells expressed ChR2 (Abbott *et al.*, 2014). In the present study, the ChR2-containing vector was delivered more rostrally to maximize expression by RTN neurons and only around 100 C1 cells expressed ChR2. Accordingly, the contribution of the C1 cells to the respiratory stimulation must have been much smaller in the present study. Also, the C1 cells are functionally heterogeneous (Guyenet *et al.*, 2013) and we do not know whether the most rostral ones are those that regulate breathing. Finally, the fiber optic was implanted caudal to the facial nucleus in the previous study (6.57±0.06 mm caudal to bregma) whereas, in the present study, fiber placement was within the coronal plane of the facial nucleus (6.13±0.03 mm caudal to bregma). This difference would also have favored the stimulation of RTN over the C1 cells given that effective stimulation requires that the tip of the optical fiber be located within 500 microns of the cell bodies. In sum, the similarities between the breathing response evoked in groups 1 and 2 likely reflect the fact that relatively few C1 cells were photoactivated in either group.

Baseline ventilation parameters after Vglut2 deletion from C1 and RTN neurons

The resting ventilatory parameters were identical in the three groups of mice. This result conforms to expectations. Resting ventilatory parameters of C57 and $D\beta H^{Cre/0}$; $Vglut2^{flox/flox}$ mice are identical (Abbott *et al.*, 2014). The total population of RTN neurons in mice is about 800 (Lazarenko *et al.*, 2009) and *Vglut2* was knocked out of fewer than half in group 3, and only on one side. Significant loss of function (chemoreflex) requires elimination of over 75 % of the RTN neurons (Takakura *et al.*, 2008; Ramanantsoa *et al.*, 2011).

RTN signals by releasing glutamate

Selective activation of the C1 cells no longer causes breathing stimulation when Vglut2 is deleted from these neurons (Abbott *et al.*, 2014). We show here that, after Vglut2 has been deleted selectively from the rostral CA cells, photoactivation of a mixture of catecholaminergic and RTN neurons still produced a robust activation of breathing (group 2). This response must therefore have resulted from the activation of ChR2-transduced RTN neurons. RTN-derived breathing stimulation was instantly maximal, consistent with the hypothesis that these cells signal with glutamate. This fast response is in sharp contrast with the slow and gradual breathing recruitment elicited, also in mice, by activating serotonergic neurons using a similar optogenetic method (Depuy *et al.*, 2011).

The breathing stimulation elicited by combined stimulation of RTN and neighboring catecholaminergic neurons was drastically reduced when Vglut2 was deleted from both neuronal types (group 3). The number of transduced RTN neurons was on average the same as in the other two groups of mice. Furthermore, the level of expression of ChR2 should have been very similar in groups 1 (Vglut2 present in both C1 and RTN neurons) and 3 (Vglut2 absent from both neuronal types) because these mice received the same combination of vectors. Accordingly, the most plausible interpretation is that glutamate release mediates the breathing stimulation elicited by RTN. This interpretation is consistent with the presence of *Vglut2* transcripts in RTN cell bodies and Vglut2 immunoreactivity in their terminals (Mulkey *et al.*, 2004; Lazarenko *et al.*, 2010; Bochorishvili *et al.*, 2012). In addition, within the ventral respiratory column, RTN neurons form asymmetric synapses with their target neurons, characteristic of excitatory glutamatergic transmission (Bochorishvili *et al.*, 2012).

An alternative interpretation of the present results deserves mention though it seems much less plausible. *Vglut2* deletion from RTN neurons could potentially cause the retraction of synapses between the affected RTN neurons and their targets within the respiratory pattern generator (plasticity hypothesis). For example, *Vglut2* deletion from dopaminergic neurons does interfere with their proper connectivity (Hnasko *et al.*, 2010; Berube-Carriere *et al.*, 2012; Fortin *et al.*, 2012). However, these changes are the consequence of deleting *Vglut2* early during development, and are therefore likely a consequence of altered development of these synapses rather than the retraction of properly formed synapses. In the present case we excised *Vglut2* from neurons that had already established their adult connections.

The small residual breathing stimulation that remained in group 3 could have resulted from the release of a transmitter other than glutamate from either RTN or a subset of catecholaminergic neurons. An equally likely explanation is the incomplete excision of *Vglut2* exon2 in the neurons that expressed the Cre recombinase because Vglut2 immunoreactivity could still be detected in approximately 9% of eYFP-positive terminals in group 3.

Finally, while the present study was being submitted, inactivation of glutamatergic synaptic transmission in a population of RTN neurons defined by intersection genetics (co-expression of Atoh1 and Phox2b) was shown to abrogate CO_2 chemosensitivity in neonatal mice (Ruffault *et al.*, 2015). These Phox2b^{on}/Atoh1^{on} neurons are very likely either the same as (or a large subset of) the Phox2b-immunoreactive neurons targeted in our study. These two

studies therefore provide congruent evidence that glutamate release is necessary for RTN neurons to **activate** breathing in conscious mice in both pups (Ruffault *et al.*, 2015) and adults (present study). This observation does not exclude the possibility that RTN might release additional transmitters whose effect might be to amplify or otherwise modulate the effect of glutamate.

Acknowledgments

This work was supported by grants from the National Institutes of Health (HL 074011 and HL028785 to PGG). We thank Chase Ford, Statistical Research Consultant for Research Data Services at the University of Virginia Library for his help with the statistics.

REFERENCES

Abbott SB, Depuy SD, Nguyen T, Coates MB, Stornetta RL, Guyenet PG. Selective optogenetic activation of rostral ventrolateral medullary catecholaminergic neurons produces cardiorespiratory stimulation in conscious mice. J. Neurosci. 2013; 33:3164–3177. [PubMed: 23407970]

Abbott SB, Holloway BB, Viar KE, Guyenet PG. Vesicular glutamate transporter 2 is required for the respiratory and parasympathetic activation produced by optogenetic stimulation of catecholaminergic neurons in the rostral ventrolateral medulla of mice in vivo. Eur. J. Neurosci. 2014; 39:98–106. [PubMed: 24236954]

Abbott SB, Stornetta RL, Coates MB, Guyenet PG. Phox2b-expressing neurons of the parafacial region regulate breathing rate, inspiration, and expiration in conscious rats. J. Neurosci. 2011; 31:16410–16422. [PubMed: 22072691]

Abbott SB, Stornetta RL, Fortuna MG, Depuy SD, West GH, Harris TE, Guyenet PG. Photostimulation of retrotrapezoid nucleus phox2b-expressing neurons in vivo produces long-lasting activation of breathing in rats. J. Neurosci. 2009; 29:5806–5819. [PubMed: 19420248]

Basting TM, Burke PG, Kanbar R, Viar KE, Stornetta DS, Stornetta RL, Guyenet PG. Hypoxia Silences Retrotrapezoid Nucleus Respiratory Chemoreceptors via Alkalosis. J. Neurosci. 2015; 35:527–543. [PubMed: 25589748]

Berube-Carriere N, Guay G, Fortin GM, Kullander K, Olson L, Wallen-Mackenzie A, Trudeau LE, Descarries L. Ultrastructural characterization of the mesostriatal dopamine innervation in mice, including two mouse lines of conditional VGLUT2 knockout in dopamine neurons. Eur. J. Neurosci. 2012; 35:527–538. [PubMed: 22330100]

Bochorishvili G, Stornetta RL, Coates MB, Guyenet PG. Pre-Botzinger complex receives glutamatergic innervation from galaninergic and other retrotrapezoid nucleus neurons. J. Comp. Neurol. 2012; 520:1047–1061. [PubMed: 21935944]

Depuy SD, Kanbar R, Coates MB, Stornetta RL, Guyenet PG. Control of breathing by raphe obscurus serotonergic neurons in mice. J. Neurosci. 2011; 31:1981–1990. [PubMed: 21307236]

Depuy SD, Stornetta RL, Bochorishvili G, Deisseroth K, Witten I, Coates MB, Guyenet PG. Glutamatergic neurotransmission between the C1 neurons and the parasympathetic preganglionic neurons of the dorsal motor nucleus of the vagus. J. Neurosci. 2013; 33:1486–1497. [PubMed: 23345223]

Dubreuil V, Thoby-Brisson M, Rallu M, Persson K, Pattyn A, Birchmeier C, Brunet JF, Fortin G, Goridis C. Defective respiratory rhythmogenesis and loss of central chemosensitivity in phox2b mutants targeting retrotrapezoid nucleus neurons. J. Neurosci. 2009; 29:14836–14846. [PubMed: 19940179]

Feldman JL, Del Negro CA, Gray PA. Understanding the rhythm of breathing: so near, yet so far. Annu. Rev. Physiol. 2013; 75:423–452. [PubMed: 23121137]

Fortin GM, Bourque MJ, Mendez JA, Leo D, Nordenankar K, Birgner C, Arvidsson E, Rymar VV, Berube-Carriere N, Claveau AM, Descarries L, Sadikot AF, Wallen-Mackenzie A, Trudeau LE. Glutamate corelease promotes growth and survival of midbrain dopamine neurons. J. Neurosci. 2012; 32:17477–17491. [PubMed: 23197738]

Gestreau C, Heitzmann D, Thomas J, Dubreuil V, Bandulik S, Reichold M, Bendahhou S, Pierson P, Sterner C, Peyronnet-Roux J, Benfriha C, Tegtmeier I, Ehnes H, Georgieff M, Lesage F, Brunet JF, Goridis C, Warth R, Barhanin J. Task2 potassium channels set central respiratory CO2 and O2 sensitivity. Proc. Natl. Acad. Sci. U.S.A. 2010; 107:2325–2330. [PubMed: 20133877]

Gourine AV, Kasymov V, Marina N, Tang F, Figueiredo MF, Lane S, Teschemacher AG, Spyer KM, Deisseroth K, Kasparov S. Astrocytes control breathing through pH-dependent release of ATP. Science. 2010; 329:571–575. [PubMed: 20647426]

Guyenet PG. Regulation of breathing and autonomic outflows by chemoreceptors. Compr. Physiol. 2014; 4:1511–1562. [PubMed: 25428853]

Guyenet PG, Mulkey DK, Stornetta RL, Bayliss DA. Regulation of ventral surface chemoreceptors by the central respiratory pattern generator. J. Neurosci. 2005; 25:8938–8947. [PubMed: 16192384]

Guyenet PG, Stornetta RL, Abbott SB, Depuy SD, Kanbar R. The retrotrapezoid nucleus and breathing. Adv. Exp. Med. Biol. 2012; 758:115–122. [PubMed: 23080151]

Guyenet PG, Stornetta RL, Bayliss DA. Central respiratory chemoreception. J. Comp. Neurol. 2010; 518:3883–3906. [PubMed: 20737591]

Guyenet PG, Stornetta RL, Bochorishvili G, Depuy SD, Burke PG, Abbott SB. C1 neurons: the body's EMTs. Am. J. Physiol. Regul. Integr. Comp. Physiol. 2013; 305:R187–204. [PubMed: 23697799]

Hawryluk JM, Moreira TS, Takakura AC, Wenker IC, Tzingounis AV, Mulkey DK. KCNQ channels determine serotonergic modulation of ventral surface chemoreceptors and respiratory drive. J. Neurosci. 2012; 32:16943–16952. [PubMed: 23175845]

Hnasko TS, Chuhma N, Zhang H, Goh GY, Sulzer D, Palmiter RD, Rayport S, Edwards RH. Vesicular glutamate transport promotes dopamine storage and glutamate corelease in vivo. Neuron. 2010; 65:643–656. [PubMed: 20223200]

Hodges MR, Richerson GB. Medullary serotonin neurons and their roles in central respiratory chemoreception. Respir. Physiol. Neurobiol. 2010

Huckstepp RT, Id BR, Eason R, Spyer KM, Dicke N, Willecke K, Marina N, Gourine AV, Dale N. Connexin hemichannel-mediated CO2-dependent release of ATP in the medulla oblongata contributes to central respiratory chemosensitivity. J. Physiol. 2010; 588:3901–3920. [PubMed: 20736421]

Hwang DY, Carlezon WA Jr. Isacson O, Kim KS. A high-efficiency synthetic promoter that drives transgene expression selectively in noradrenergic neurons. Hum. Gene Ther. 2001; 12:1731–1740. [PubMed: 11560767]

Kam K, Worrell JW, Ventalon C, Emiliani V, Feldman JL. Emergence of population bursts from simultaneous activation of small subsets of preBotzinger complex inspiratory neurons. J. Neurosci. 2013; 33:3332–3338. [PubMed: 23426661]

Kaur S, Pedersen NP, Yokota S, Hur EE, Fuller PM, Lazarus M, Chamberlin NL, Saper CB. Glutamatergic signaling from the parabrachial nucleus plays a critical role in hypercapnic arousal. J. Neurosci. 2013; 33:7627–7640. [PubMed: 23637157]

Kumar NN, Velic A, Soliz J, Shi Y, Li K, Wang S, Weaver JL, Sen J, Abbott SBG, Lazarenko RM, Ludwig M-G, Perez-Reyes E, Mohebbi N, Bettoni C, Gassmann M, Suply T, Seuwen K, Guyenet PG, Wagner CA, Bayliss DA. Regulation of breathing by CO2 requires the proton-activated receptor GPR4 in retrotrapezoid nucleus neurons. Science. 2015 In press.

Lazarenko RM, Fortuna MG, Shi Y, Mulkey DK, Takakura AC, Moreira TS, Guyenet PG, Bayliss DA. Anesthetic activation of central respiratory chemoreceptor neurons involves inhibition of a THIK-1-like background K(+) current. J. Neurosci. 2010; 30:9324–9334. [PubMed: 20610767]

Lazarenko RM, Milner TA, Depuy SD, Stornetta RL, West GH, Kievits JA, Bayliss DA, Guyenet PG. Acid sensitivity and ultrastructure of the retrotrapezoid nucleus in Phox2b-EGFP transgenic mice. J. Comp. Neurol. 2009; 517:69–86. [PubMed: 19711410]

Li A, Nattie E. Antagonism of rat orexin receptors by almorexant attenuates central chemoreception in wakefulness in the active period of the diurnal cycle. J. Physiol. 2010; 588:2935–2944. [PubMed: 20547681]

Lin W, McKinney K, Liu L, Lakhlani S, Jennes L. Distribution of vesicular glutamate transporter-2 messenger ribonucleic Acid and protein in the septum-hypothalamus of the rat. Endocrinology. 2003; 144:662–670. [PubMed: 12538629]

Marina N, Abdala AP, Trapp S, Li A, Nattie EE, Hewinson J, Smith JC, Paton JF, Gourine AV. Essential role of Phox2b-expressing ventrolateral brainstem neurons in the chemosensory control of inspiration and expiration. J. Neurosci. 2010; 30:12466–12473. [PubMed: 20844141]

Mulkey DK, Stornetta RL, Weston MC, Simmons JR, Parker A, Bayliss DA, Guyenet PG. Respiratory control by ventral surface chemoreceptor neurons in rats. Nat. Neurosci. 2004; 7:1360–1369. [PubMed: 15558061]

Nattie E, Li A. Central chemoreception in wakefulness and sleep: evidence for a distributed network and a role for orexin. J. Appl. Physiol. 2010; 108:1417–1424. [PubMed: 20133433]

Onimaru H, Homma I. A novel functional neuron group for respiratory rhythm generation in the ventral medulla. J. Neurosci. 2003; 23:1478–1486. [PubMed: 12598636]

Pattyn A, Morin X, Cremer H, Goridis C, Brunet JF. Expression and interactions of the two closely related homeobox genes Phox2a and Phox2b during neurogenesis. Development. 1997; 124:4065–4075. [PubMed: 9374403]

Pieribone VA, Xu ZQ, Zhang X, Hokfelt T. Electrophysiologic effects of galanin on neurons of the central nervous system. Ann.N.Y.Acad.Sci. 1998; 863:264–273. [PubMed: 9928177]

Ramanantsoa N, Hirsch MR, Thoby-Brisson M, Dubreuil V, Bouvier J, Ruffault PL, Matrot B, Fortin G, Brunet JF, Gallego J, Goridis C. Breathing without CO2 chemosensitivity in conditional Phox2b mutants. J. Neurosci. 2011; 31:12880–12888. [PubMed: 21900566]

Rosin DL, Weston MC, Sevigny CP, Stornetta RL, Guyenet PG. Hypothalamic orexin (hypocretin) neurons express vesicular glutamate transporters VGLUT1 or VGLUT2. J. Comp. Neurol. 2003; 465:593–603. [PubMed: 12975818]

Ruffault PL, D'Autreaux F, Hayes JA, Nomaksteinsky M, Autran S, Fujiyama T, Hoshino M, Hagglund M, Kiehn O, Brunet JF, Fortin G, Goridis C. The retrotrapezoid nucleus neurons expressing Phox2b and Atoh-1 are essential for the respiratory response to CO2. Elife. 2015; 4 doi: 10.7554/eLife.07051.

Smith JC, Morrison DE, Ellenberger HH, Otto MR, Feldman JL. Brainstem projections to the major respiratory neuron populations in the medulla of the cat. J.Comp.Neurol. 1989; 281:69–96. [PubMed: 2466879]

Stornetta RL, Moreira TS, Takakura AC, Kang BJ, Chang DA, West GH, Brunet JF, Mulkey DK, Bayliss DA, Guyenet PG. Expression of Phox2b by brainstem neurons involved in chemosensory integration in the adult rat. J. Neurosci. 2006; 26:10305–10314. [PubMed: 17021186]

Stornetta RL, Sevigny CP, Schreihofer AM, Rosin DL, Guyenet PG. Vesicular glutamate transporter DNPI/GLUT2 is expressed by both C1 adrenergic and nonaminergic presympathetic vasomotor neurons of the rat medulla. J. Comp. Neurol. 2002; 444:207–220. [PubMed: 11840475]

Stornetta RL, Spirovski D, Moreira TS, Takakura AC, West GH, Gwilt JM, Pilowsky PM, Guyenet PG. Galanin is a selective marker of the retrotrapezoid nucleus in rats. J. Comp. Neurol. 2009; 512:373–383. [PubMed: 19006184]

Stuber GD, Hnasko TS, Britt JP, Edwards RH, Bonci A. Dopaminergic terminals in the nucleus accumbens but not the dorsal striatum corelease glutamate. J. Neurosci. 2010; 30:8229–8233. [PubMed: 20554874]

Takakura AC, Moreira TS, Stornetta RL, West GH, Gwilt JM, Guyenet PG. Selective lesion of retrotrapezoid Phox2b-expressing neurons raises the apnoeic threshold in rats. J. Physiol. 2008; 586:2975–2991. [PubMed: 18440993]

Takamori S, Rhee JS, Rosenmund C, Jahn R. Identification of a vesicular glutamate transporter that defines a glutamatergic phenotype in neurons. Nature. 2000; 407:189–194. [PubMed: 11001057]

Tong Q, Ye C, McCrimmon RJ, Dhillon H, Choi B, Kramer MD, Yu J, Yang Z, Christiansen LM, Lee CE, Choi CS, Zigman JM, Shulman GI, Sherwin RS, Elmquist JK, Lowell BB. Synaptic glutamate release by ventromedial hypothalamic neurons is part of the neurocircuitry that prevents hypoglycemia. Cell Metab. 2007; 5:383–393. [PubMed: 17488640]

Van den Pol AN. Neuropeptide transmission in brain circuits. Neuron. 2012; 76:98–115. [PubMed: 23040809]

Wang S, Benamer N, Zanella S, Kumar NN, Shi Y, Bevengut M, Penton D, Guyenet PG, Lesage F, Gestreau C, Barhanin J, Bayliss DA. TASK-2 channels contribute to pH sensitivity of

retrotrapezoid nucleus chemoreceptor neurons. J. Neurosci. 2013a; 33:16033–16044. [PubMed: 24107938]

Wang S, Shi Y, Shu S, Guyenet PG, Bayliss DA. Phox2b-expressing retrotrapezoid neurons are intrinsically responsive to acidification and CO_2. J. Neurosci. 2013b; 33:7756–7761. [PubMed: 23637167]

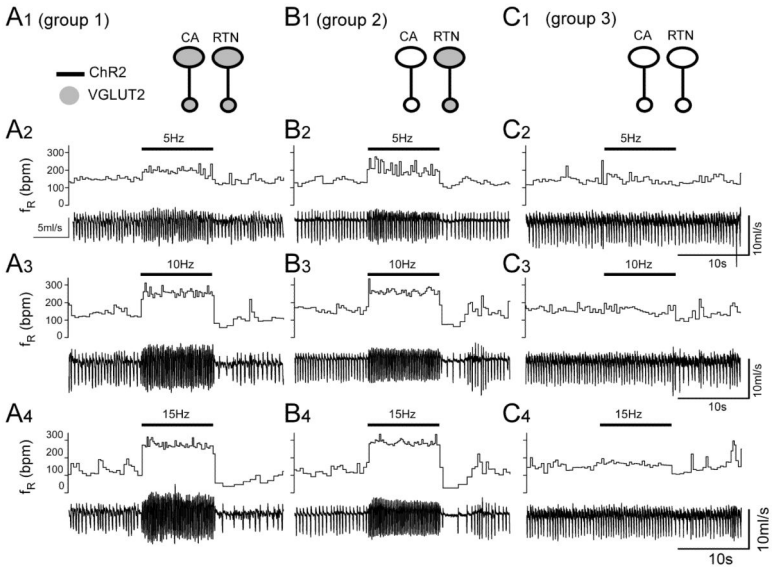

Figure 1. Breathing stimulation elicited by combined optogenetic activation of RTN and C1 neurons in mice in which *Vglut2* was deleted from the C1 neurons or from both RTN and C1 neurons

A1-A4: photostimulation of a mix of ChR2-transduced RTN and C1 neurons in control mice (C57). Unilateral stimulation was done in conscious mice using trains of 5 ms-long light pulses delivered at 5, 10 or 15 Hz. In each panel, the bottom trace is the raw plethysmography signal (airflow with inspiration downward) and the top trace is the breathing frequency. Note the immediate and sustained increase in breathing frequency. The apnea that follows the stimulation period is likely caused by the reduction in arterial PCO_2 consecutive to the hyperventilation. B1-B4: same experiment in a group 2 mouse in which ChR2-transduced C1 neurons no longer express Vglut2 but RTN neurons still express this vesicular transporter. C1-C4: same experiment in a group 3 mouse in which few or none of the ChR2-transduced neurons express Vglut2. Note the almost complete loss of the breathing response.

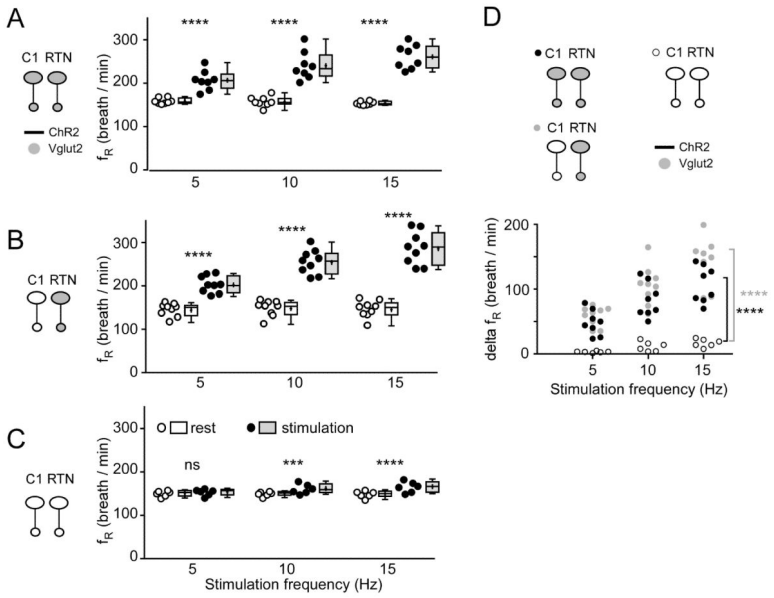

Figure 2. Optogenetic activation of RTN and C1 neurons: effect on breathing frequency

A. Breathing frequency (f_R) at rest (open circles represent individual data points and box and whisker plots summarize each data set with means indicated by crosses) and during photostimulation (black circles and gray boxes) in control mice. In these mice Vglut2 is expressed by both types of ChR2-tranasduced neurons (C1 and RTN). B. Breathing frequency (f_R) at rest (open circles and boxes) and during photostimulation (black circles and gray boxes) in mice in which ChR2-transduced RTN express Vglut2 but ChR2-transduced C1 cells do not express Vglut2. C. Breathing frequency (f_R) at rest (open circles and boxes) and during photostimulation (black circles and gray boxes) of neurons in mice in which neither C1 nor RTN ChR2-transduced neurons express Vglut2. D. change in breathing frequency produced by photostimulating ChR2-transduced neurons in the three mice groups.

In A-C *** $P = 0.0003$ and **** $P < 0.0001$ (post hoc Sidak multiple comparison between rest and stimulation). In D, **** $P < 0.0001$ (between group 3 and groups 1 or 2 at 15 Hz by Tukey's post hoc multiple comparison test between groups, see Table 4 for q and P values).

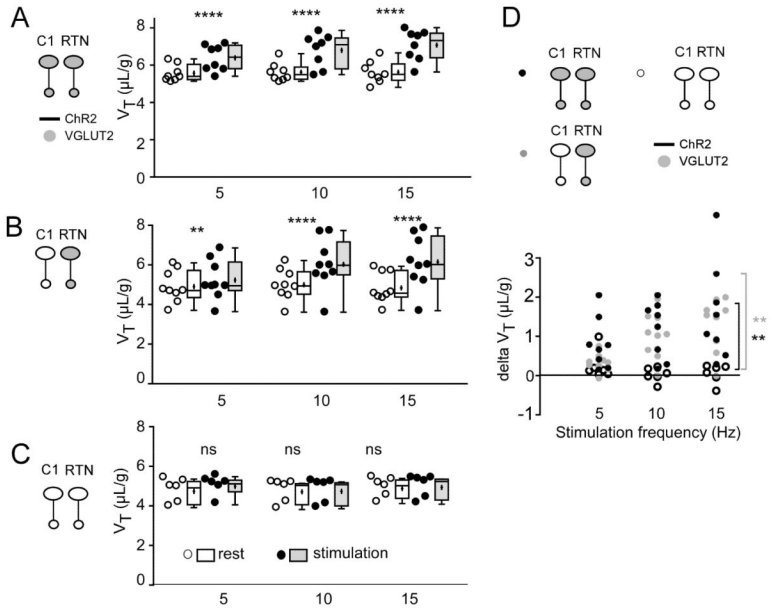

Figure 3. Optogenetic activation of RTN and C1 neurons: effect on tidal volume (V_T)

The data is presented as in Figure 2. A-C. V_T at rest (open circles represent individual data points and box and whisker plots summarize each data set with means indicated by crosses) and during photostimulation (black circles and gray boxes) in control mice (A, group 1), in mice in which ChR2-transduced RTN express Vglut2 but ChR2-transduced C1 cells do not express Vglut2 (B, group 2) and in mice in which neither C1 nor RTN ChR2-transduced neurons express Vglut2 (C, group 3). D. changes in V_T produced by photostimulating ChR2-transduced neurons in the three mice groups.

In A-C ** $P = 0.0097$ and **** $P < 0.0001$ (post hoc Sidak multiple comparison tests between rest and stimulation). In D, ** $P < 0.01$ (between group 3 and groups 1 or 2 at 15 Hz by Tukey's post hoc multiple comparison test between groups, see Table 4 for q and exact P values).

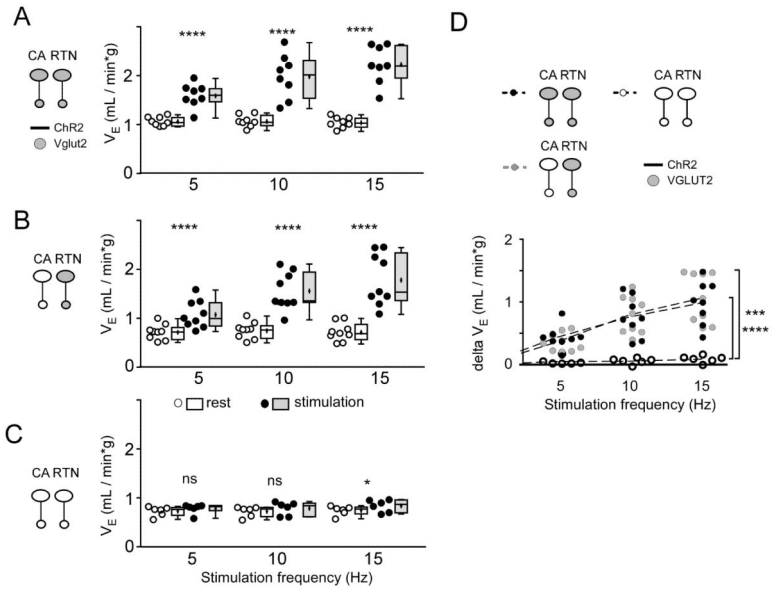

Figure 4. Optogenetic activation of RTN and CA neurons: effect on minute volume (V_E)

The data is presented as in Figure 2. A-C. Minute volume ($V_E = f_R \times V_T$) at rest (open circles and boxes) and during photostimulation (black circles and gray boxes) in control mice (A, group 1), in mice in which ChR2-transduced RTN express Vglut2 but ChR2-transduced C1 cells do not express Vglut2 (B, group 2) and in mice in which neither CA nor RTN ChR2-transduced neurons express Vglut2 (C, group 3). D. changes in V_E produced by photostimulating ChR2-transduced neurons in the three mice groups.

In A-C * $P = 0.0161$ and **** $P < 0.0001$ (Sidak post hoc multiple comparisons). In D, *** $P = 0.0002$ and **** $P < 0.0001$ (between group 3 and groups 1 or 2 at 15 Hz by Tukey's post hoc multiple comparison test between groups, see Table 4 for *q* and P values).

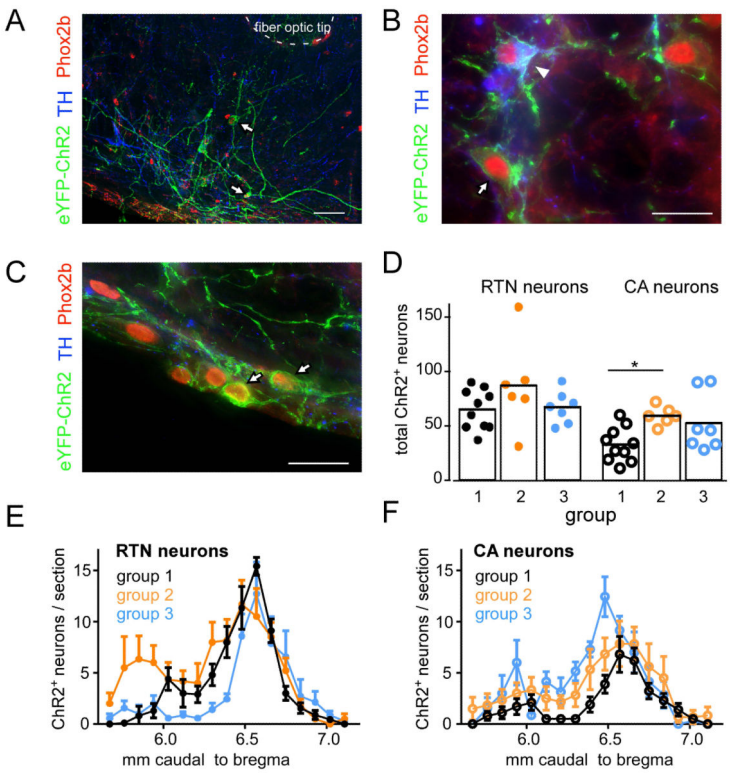

Figure 5. PRSx8-ChR2-eYFP LVV selectively transduces Phox2b-expressing neurons

A. Transverse section through the rostral ventrolateral medulla at the level of the posterior edge of the facial motor nucleus (FN). The ventral surface of the medulla is showing at the lower left corner. All the ChR2-eYFP transduced neurons (black-rimmed white arrows) have Phox2b-immunoreactive nuclei. The section also shows the location of the tip of the optical fiber that was implanted to photoactivate the ChR2-expressing neurons. B. Side by side example of a ChR2-transduced catecholaminergic neuron (TH-immunoreactive; white arrowhead) and a ChR2-transduced RTN neuron (TH-negative; black-rimmed white arrow). Both neurons contain plasma membrane-associated eYFP and a Phox2b-immunoreactive nucleus. The catecholaminergic neurons also contains TH. C. Typical example of RTN neurons (positive for Phox2b-and ChR2-eYFP but TH-negative) lining the ventral surface of the brainstem ventral to the facial motor nucleus. D-F. Rostro-caudal distribution of ChR2-transduced RTN and catecholaminergic neurons in the three experimental groups. More RTN than CA neurons were transduced with ChR2-eYFP although all experimental groups were transduced with similar populations of these neurons. Scale bar in A, 50 μm; in B and C, 20 μm.

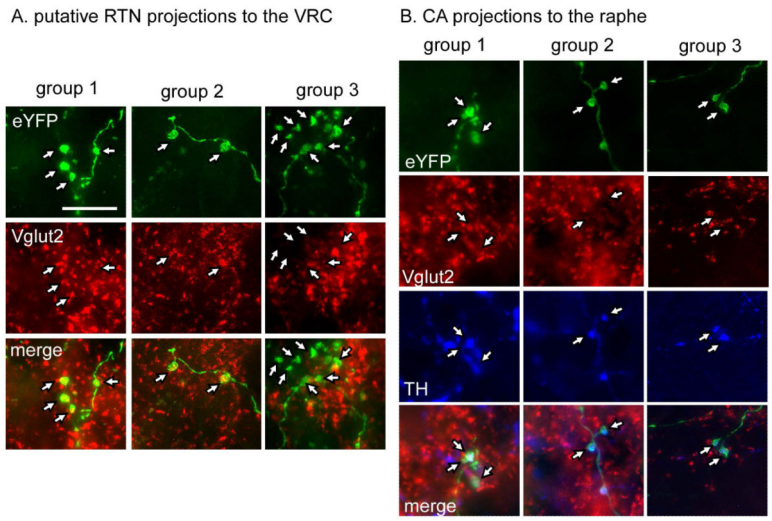

Figure 6. Appropriate deletion of Vglut2 from RTN and CA terminals

A. eYFP-positive terminals from RTN injections seen in the ventral respiratory column (vrc) are Vglut2 positive in groups 1 and 2 but lack Vglut2 immunoreactivity in group 3.

B. eYFP-positive terminals in raphe pallidus from catecholaminergic neurons (CA, defined by their tyrosine hydroxylase (TH) immunoreactivity) contain Vglut2 in group 1 but lack Vglut2 in groups 2 and 3. Scale bar = 10 μm.

Table 1

Experimental design

Group	Mouse	Vector(s)	C1 cells	R N cells	Breathing stimulation
1	*DβH*$^{+/+}$;;*Vglut2*$^{+/+}$ (C57)	PRSx8-Cre LV + DIO-ChR2-eYFP AAV	ChR2+/Vglut2+	ChR2+/Vglut2+	Yes^{+}
2	*DβH*$^{Cre/0}$;;*Vglut2*$^{fl/fl}$	PRSx8-ChR2-eYFP LV	ChR2+/Vglut2−	ChR2+/Vglut2+	Yes^{+}
3	*DβH*$^{+/+}$;;*Vglut2*$^{fl/fl}$	PRSx8-Cre LV + DIO-ChR2-eYFP AAV	ChR2+/Vglut2−	ChR2+/Vglut2−	No^{+}

Groups 1-3: new experiments performed in the present study.

$^{+}$ expected result if selective stimulation of RTN neurons increases breathing by releasing glutamate.

Table 2

Shapiro-Wilk Statistics

Shapiro Wilk test statistics on residuals for 2 WAY RM ANOVA						
	f_R within	f_R between	V_T within	V_T between	V_E within	V_E between
Group 1 effect of stim freq × before/during stim N = 8	W = 0.9514 *P* = 0.742	W = 0.9460 *P* = 0.4292	W = .9235 *P* = 0.4973	W = 0.9352 *P* = 0.2941	W = 0.8276 *P* = 0.0760	W = 0.9322 *P* = 0.2644
Group 2 effect of stim freq × before/during stim N = 9	W = 0.9142 *P* = 0.3849	W = 0.9725 *P* = 0.8436	W = 0.9795 *P* = 0.9604	W = 0.9462 *P* = 0.3683	W = 0.9420 *P* = 0.6305	W = 0.9812 *P* = 0.9612
Group 3 effect of stim freq × before/during stim N= 6	W = 0.9682 *P* = 0.8638	W = 0.9825 *P*= 0.9918	W = .8450 *P* = 0.1793	W = 0.9587 *P* = 0.7657	W = .7763 *P* = .05119	W = 0.8737 *P* = 0.0728
delta stim w groups × freq of stim	W = 0.9483 *P* = 0.0404*	W = 0.9635 *P* = 0.5642	W = 0.9936 *P* = 0.9964	W = 0.8723 *P* = 0.008*	W = 0.9738 *P* = 0.3792	W = 0.9593 *P* = 0.4758
Shapiro-Wilk test statistic on residuals for One-Way ANOVA for all groups at baseline						
	f_R		V_T		V_E	
Baseline on groups	W = 0.93006 *P* = 0.1097		W = 0.97722 *P* = 0.8538		W = 0.97501 *P* = 0.8065	
Shapiro-Wilk test statistic on residuals for One-Way ANOVA for all groups at 15 Hz stimulation						
delta stim @ 15 hz on 3 groups	W = 0.9810 *P* = 0.9206		W = 0.9748 *P* = 0.8011		W = 0.94447 *P* = 0.2239	

Table 3

F statistics

F-test statistics for Two-Way ANOVAs						
test/ group	main effect of stim (before/during)	main effect of stim frequency	main effect of stim (before/during)	main effect of stim frequency	main effect of stim (before/during)	main effect of stim frequency
	f_R		V_T		V_E	
Group 1 N=8 RM on both before/during and freq of stim	$F_{1, 7}$ = 87.77 P < 0.0001	$F_{2, 14}$ = 26.19 P < 0.0001	$F_{1, 7}$ = 20.92 P = 0.0026	$F_{2, 14}$ = 7.664 P = 0.0056	$F_{1, 7}$ = 57.31 P = 0.0001	$F_{2, 14}$ = 23.97 P < 0.0001
Group 2 N=9 RM on both before/during and freq of stim	$F_{1, 8}$ = 133.4 P < 0.0001	$F_{2, 16}$ = 91.76 P < 0.0001	$F_{1, 8}$ = 30.65 P = 0.0005	$F_{2, 16}$ = 12.97 P = 0.0004	$F_{1, 8}$ = 65.28 P < 0.0001	$F_{2, 16}$ = 41.05 P < 0.0001
Group 3 N=6 RM on both before/during and freq of stim	$F_{1, 5}$ = 34.71 P = 0.0020	$F_{2, 10}$ = 2.027 P = 0.1824	$F_{1, 5}$ = 11.72 P = 0.0188	$F_{2, 10}$ = 2.395 P = 0.1413	$F_{1, 5}$ = 114.4, P = 0.0001	$F_{2,10}$ = 1.858 P = 0.206
	main effect of group for V_E	main effect of stim frequency for V_E				
delta stim w groups × freq (RM on freq)	$F_{2,20}$ = 17.48, P = 4.07e-05	$F_{2,40}$ = 84.22, P = 4.59e-15				
F test statistics for One-Way ANOVA for all groups at baseline						
	f_R		V_T		V_E	
Baseline breathing on groups	$F_{2,20}$ = 1.452 P = 0.258		$F_{2,20}$ = 3.05 P = 0.0698		$F_{2,20}$ = 3.489 P = 0.0501	
F test statistics for One-Way ANOVA for all groups at 15 hz stimulation						
	f_R		V_T		V_E	
delta stim @ 15 hz on groups	$F_{2,20}$ = 34.3 P = 3.43e-07		$F_{2,20}$ = 7.826 P= 0.00309		$F_{2,20}$ = 18.42 P = 2.91e-05	

Table 4

Tukey's multiple comparison test statistics for all group differences at 15 Hz stimulation.

	f_R		V_T		V_E	
	q* and *P	**95% confidence interval**	***q* and *P***	**95% confidence interval**	***q* and *P***	**95% confidence interval**
Group 1vs. Group 2	q_{20} = 3.351 P = 0.0690	−68.35 to 2.242	q_{20} = 0.6241 P = 0.8987	−0.7192 to 1.023	q_{20} = 0.6947 P = 0.8763	−0.4797 to 0.3237
Group 1 vs. Group 3	q_{20} = 8.273 P < 0.0001	51.47 to 129.9	q_{20} = 5.186 P = 0.0042	0.4351 to 2.372	q_{20} = 7.191 P = 0.0002	0.4509 to 1.344
Group 2 vs. Group 3	q_{20} = 11.57 P < 0.0001	85.47 to 162.0	q_{20} = 4.739 P = 0.0085	0.3065 to 2.196	q_{20} = 8.009 P < 0.0001	0.5397 to 1.411